Generation of a Magnetic Field by Dynamo Action in a Turbulent Flow of Liquid Sodium

R. Monchaux,[1] M. Berhanu,[2] M. Bourgoin,[3,*] M. Moulin,[3] Ph. Odier,[3] J.-F. Pinton,[3] R. Volk,[3] S. Fauve,[2] N. Mordant,[2] F. Pétrélis,[2] A. Chiffaudel,[1] F. Daviaud,[1] B. Dubrulle,[1] C. Gasquet,[1] L. Marié,[1,†] and F. Ravelet[1,‡]

[1]*Service de Physique de l'Etat Condensé, Direction des Sciences de la Matière, CEA-Saclay, CNRS URA 2464, 91191 Gif-sur-Yvette cedex, France*

[2]*Laboratoire de Physique Statistique de l'Ecole Normale Supérieure, CNRS UMR 8550, 24 Rue Lhomond, 75231 Paris Cedex 05, France*

[3]*Laboratoire de Physique de l'Ecole Normale Supérieure de Lyon, CNRS UMR 5672, 46 allée d'Italie, 69364 Lyon Cedex 07, France*

(Received 25 October 2006; published 25 January 2007)

We report the observation of dynamo action in the von Kármán sodium experiment, i.e., the generation of a magnetic field by a strongly turbulent swirling flow of liquid sodium. Both mean and fluctuating parts of the field are studied. The dynamo threshold corresponds to a magnetic Reynolds number $R_m \sim 30$. A mean magnetic field of the order of 40 G is observed 30% above threshold at the flow lateral boundary. The rms fluctuations are larger than the corresponding mean value for two of the components. The scaling of the mean square magnetic field is compared to a prediction previously made for high Reynolds number flows.

DOI: 10.1103/PhysRevLett.98.044502 PACS numbers: 47.65.−d, 52.65.Kj, 91.25.Cw

The generation of electricity from mechanical work was one of the main achievements of physics at the end of the 19th century. In 1919, Larmor proposed that a similar process could generate the magnetic field of the Sun from the motion of an electrically conducting fluid. However, fluid dynamos are more complex than industrial ones and it is not easy to find laminar flow configurations that generate magnetic fields [1]. Two simple but clever examples were found in the 1970s [2] and have led more recently to successful experiments [3]. These experiments have shown that the observed thresholds are in good agreement with theoretical predictions [4] made by considering only the mean flow, whereas the saturation level of the magnetic field cannot be described with a laminar flow model (without using an *ad hoc* turbulent viscosity) [5]. These observations have raised many questions: what happens for flows without geometrical constraints such that fluctuations are of the same order of magnitude as the mean flow? Is the dynamo threshold strongly increased due to the lack of coherence of the driving flow [6,7] or does the prediction made as if the mean flow were acting alone still give a reasonable order of magnitude [8]? What is the nature of the dynamo bifurcation in the presence of large velocity fluctuations? All of these questions, and others motivated by geophysical or astrophysical dynamos [9], have led several teams to try to generate dynamos in flows with a high level of turbulence [10,11]. We present in this Letter our first experimental observation of the generation of a magnetic field in a von Kármán swirling flow of liquid sodium (VKS) for which velocity fluctuations and the mean flow have comparable kinetic energy and we discuss some of the above issues. The experimental setup (see Fig. 1) is similar to the previous VKS experiments [11], but involves three modifications that will be described below. The flow is generated by rotating two disks of radius 154.5 mm, 371 mm apart in a cylindrical vessel, $2R =$ 412 mm in inner diameter and 524 mm in length. The disks are fitted with 8 curved blades of height $h = 41.2$ mm. These impellers are driven at a rotation frequency up to $\Omega/2\pi = 26$ Hz by 300 kW available motor power. An oil circulation in the outer copper cylinder maintains a regulated temperature in the range 110–160 °C. The mean flow has the following characteristics: the fluid is ejected radially outward by the disks; this drives an axial flow toward the disks along their axis and a recirculation in the opposite direction along the cylinder lateral boundary. In addition, in the case of counterrotating disks studied here, the presence of a strong axial shear of azimuthal velocity in the midplane between the impellers generates a high level of turbulent fluctuations [12,13]. The kinetic Reynolds num-

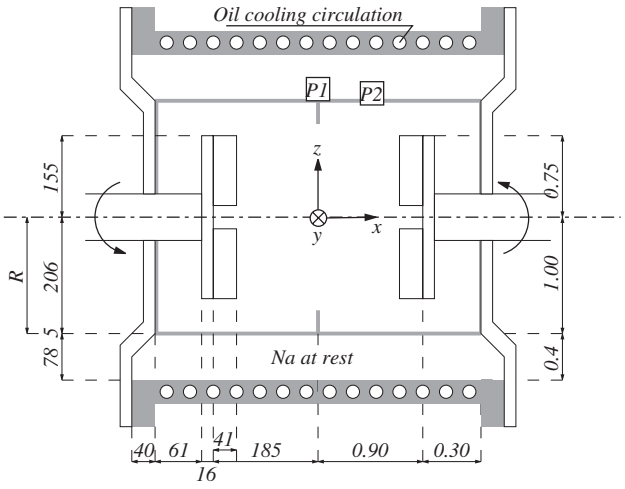

FIG. 1. Sketch of the experimental setup. The inner and outer cylinders are made of copper (in gray). The dimension are given in millimeter (left) and normalized by R (right). The 3D Hall probe is located either at point $P1$ in the midplane or $P2$. In both cases, the probe is nearly flush with the inner shell.

ber is $\mathrm{Re} = KR^2\Omega/\nu$, where ν is the kinematic viscosity and $K = 0.6$ is a coefficient that measures the efficiency of the impellers [14]. Re can be increased up to 5×10^6: the corresponding magnetic Reynolds number is $R_m = K\mu_0\sigma R^2\Omega \approx 49$ (at 120 °C), where μ_0 is the magnetic permeability of vacuum and σ is the electrical conductivity of sodium.

A first modification with respect to earlier VKS experiments consists of surrounding the flow by sodium at rest in another concentric cylindrical vessel, 578 mm in inner diameter. This has been shown to decrease the dynamo threshold in kinematic computations based on the mean flow velocity [14]. The total volume of liquid sodium is 150 l. A second geometrical modification consists of attaching an annulus of inner diameter 175 mm and thickness 5 mm along the inner cylinder in the midplane between the disks. Water experiments have shown that its effect on the mean flow is to make the shear layer sharper around the midplane. In addition, it reduces low frequency turbulent fluctuations, thus the large scale flow time-averages faster toward the mean flow. However, rms velocity fluctuations are almost unchanged (of order 40%–50%), thus the flow remains strongly turbulent [15]. It is expected that reducing the transverse motion of the shear layer decreases the dynamo threshold for the following reasons: (i) magnetic induction due to an externally applied field on a gallium flow strongly varies because of the large scale flow excursions away from the time averaged flow [16], (ii) the addition of large scale noise to the Taylor-Green mean flow increases its dynamo threshold [7], (iii) fluctuating motion of eddies increase the dynamo threshold of the Roberts flow [17].

The above configuration does not generate a magnetic field up to the maximum possible rotation frequency of the disks ($\Omega/2\pi = 26$ Hz). We thus made a last modification and replaced disks made of stainless steel by similar iron disks. Using boundary conditions with a high permeability in order to change the dynamo threshold has been already proposed [18]. It has been also shown that in the case of a Ponomarenko or G. O. Roberts flows, the addition of an external wall of high permeability can decrease the dynamo threshold [19]. Finally, recent kinematic simulations of the VKS mean flow have shown that different ways of taking into account the sodium behind the disks lead to an increase of the dynamo threshold ranging from 12% to 150% [20]. We thought that using iron disks could screen magnetic effects in the bulk of the flow from the region behind the disks, although the actual behavior may be more complex. This last modification generates a dynamo above $R_m \simeq 30$. The three components of the field $\vec{B}$ are measured with a 3D Hall probe, located either in the midplane or 109 mm away from it ($P1$ or $P2$ in Fig. 1). In both cases, the probe is nearly flush with the inner shell, thus $\vec{B}$ is measured at the boundary of the turbulent flow. Figure 2 shows the time recording of the three components of $\vec{B}$ when R_m is increased from 19 to 40. The largest component

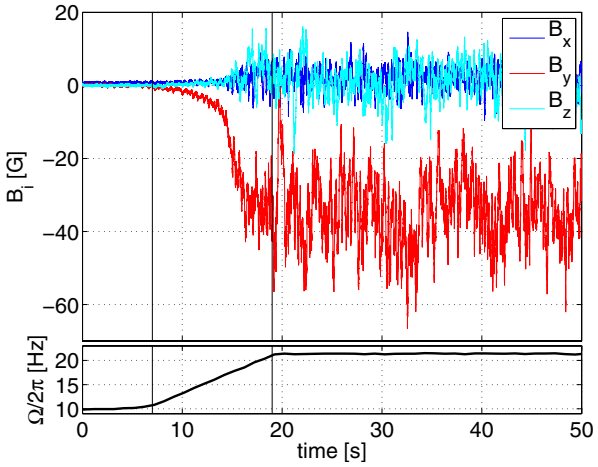

FIG. 2 (color online). Time recording at $P1$ of the components of the magnetic field when the rotation frequency $\Omega/2\pi$ is increased as displayed by the ramp below (R_m increases from 19 to 40).

B_y is tangent to the cylinder at the measurement location. It increases from a mean value comparable to the Earth magnetic field to roughly 40 G. The mean values of the other components B_x and B_z also increase (not visible on the figure because of fluctuations). Both signs of the components have been observed in different runs, depending on the sign of the residual magnetization of the disks. All components display strong fluctuations as could be expected in flows with Reynolds numbers larger than 10^6.

Figure 3(a) shows the mean values of the components $\langle B_i \rangle$ of the magnetic field and Fig. 3(b) their fluctuations $B_{i\mathrm{rms}}$ versus R_m. The fluctuations are all in the same range (3 to 8 G, at 30% above threshold) although the corresponding mean values are very different. The time average of the square of the total magnetic field, $\langle \vec{B}^2 \rangle$, is displayed in the inset of Fig. 3(a). No hysteresis is observed. Linear fits of $\langle B_y \rangle$ or $B_{i\mathrm{rms}}$ displayed in Fig. 3 define a critical magnetic Reynolds number $R_m^c \sim 31$ whereas the linear fit of $\langle \vec{B}^2 \rangle$ gives a larger value $R_m^0 \sim 35$. The latter is the one that should be considered in the case of a supercritical pitchfork bifurcation. The rounding observed close to threshold could then be ascribed to the imperfection due to the ambient magnetic field (Earth field, residual magnetization of the disks and other magnetic perturbations of the setup). The actual behavior may be more complex because this bifurcation takes place on a strongly turbulent flow, a situation for which no rigorous theory exists. The inset of Fig. 3(b) shows that the variance $B_{\mathrm{rms}}^2 = \langle (\vec{B} - \langle \vec{B} \rangle)^2 \rangle$ is not proportional to $\langle B^2 \rangle$. Below the dynamo threshold, the effect of induction due to the ambient magnetic field is observed. $B_{\mathrm{rms}}/\langle B^2 \rangle^{1/2}$ first behaves linearly at low R_m, but then increases faster as R_m becomes closer to the bifurcation threshold. We thus show that this seems to be a good quantity to look at as a precursor of a dynamo regime. In addition, we observe that it displays a discontinuity in slope in the vicinity of R_m^c in an analogous way of some

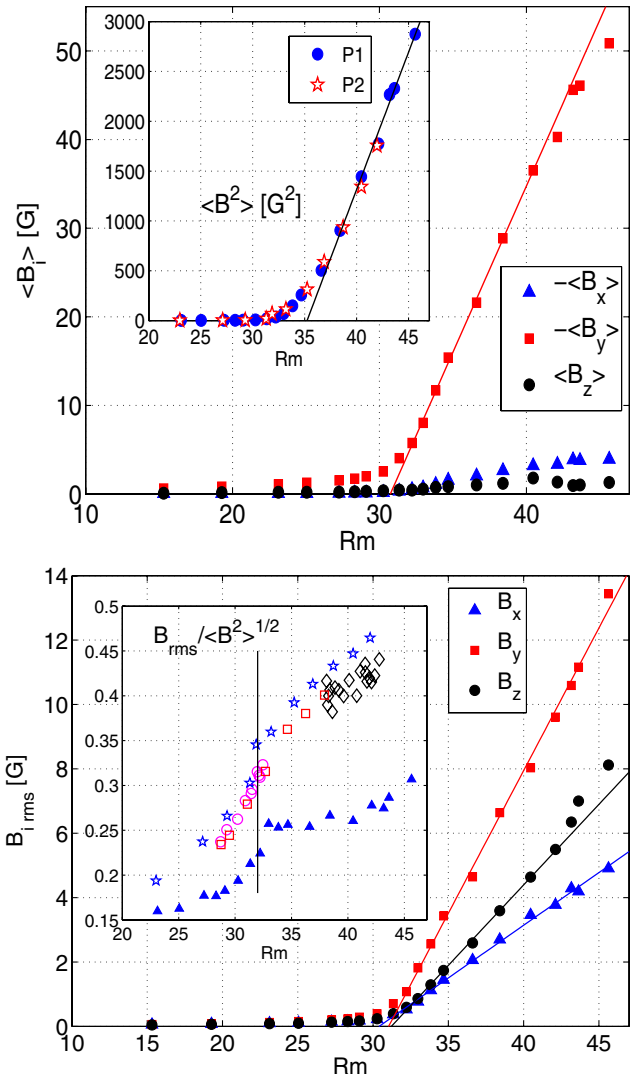

FIG. 3 (color online). (a) Mean values of the three components of the magnetic field recorded at $P1$ versus R_m ($T = 120\,^{\circ}\mathrm{C}$): (▲) $-\langle B_x\rangle$, (■) $-\langle B_y\rangle$, (●) $\langle B_z\rangle$. The inset shows the time average of the square of the total magnetic field as a function of R_m, measured at $P1$ (●), or at $P2$ (★) after being divided by 1.8. (b) Standard deviation of the fluctuations of each components of the magnetic field recorded at $P1$ versus R_m. The inset shows $B_{\mathrm{rms}}/\langle B^2\rangle^{1/2}$. Measurements done at $P1$: (▲) $T = 120\,^{\circ}\mathrm{C}$, frequency increased up to 22 Hz; Measurements done at $P2$: (★) $T = 120\,^{\circ}\mathrm{C}$, frequency decreased from 22 to 16.5 Hz, (□) $T = 156\,^{\circ}\mathrm{C}$, frequency increased up to 22 Hz, (○) $\Omega/2\pi = 16.5$ Hz, T varied from 154 to 116 °C, (◇) $\Omega/2\pi = 22$ Hz, T varied from 119 to 156 °C. The vertical line corresponds to $R_m = 32$.

response functions at phase transitions or bifurcations in the presence of noise. Note, however, that the shape of the curves depends on the measurement point and they cannot be superimposed with a scaling factor as done for $\langle B^2\rangle$ versus R_m in the inset of Fig. 3(a).

The above results are characteristic of bifurcations in the presence of noise. As shown in much simpler experiments, different choices of an order parameter (mean value of the amplitude of the unstable mode or its higher moments, its most probable value, etc.) can lead to qualitatively different bifurcation diagrams [21]. This illustrates the ambiguity in the definition of the order parameter for bifurcations in the presence of fluctuations or noise. In the present experiment, fluctuations enter both multiplicatively, because of the turbulent velocity, and additively, due to the interaction of the velocity field with the ambient magnetic field. Finally, we note that both R_m^c and R_m^0 are smaller than the thresholds computed with kinematic dynamo codes taking into account only the mean flow, that are in the range $R_m^c = 43$ to 150 depending on different boundary conditions on the disks and on configurations of the flow behind them [14,20].

The probability density functions (PDF) of the fluctuations of the three components of the induced magnetic field (not displayed) are roughly Gaussian. The PDFs of fluctuations below threshold, i.e., due to the induction resulting from the ambient magnetic field, are similar to the ones observed in the self-generating regime. We do not observe any non-Gaussian behavior close to threshold which would result from an on-off intermittency mechanism [22]. Possible reasons are the low level of small frequency velocity fluctuations [23] or the imperfection of the bifurcation that results from the ambient magnetic field [24].

Figure 4 displays both the dimensional (see inset) and dimensionless mean square field as a function of R_m. $\langle B^2\rangle$ is made dimensionless using a high Reynolds number scaling [5]: $\langle B^2\rangle \propto \rho/(\mu_0(\sigma R)^2)(R_m - R_m^c)/R_m^c$, where ρ is the fluid density. We observe that data obtained at different working temperature are well collapsed by this scaling (σ decreases by roughly 15% from 100 to 160 °C). The low Reynolds number or "weak field" scaling could also give a reasonable collapse of data obtained on this tem-

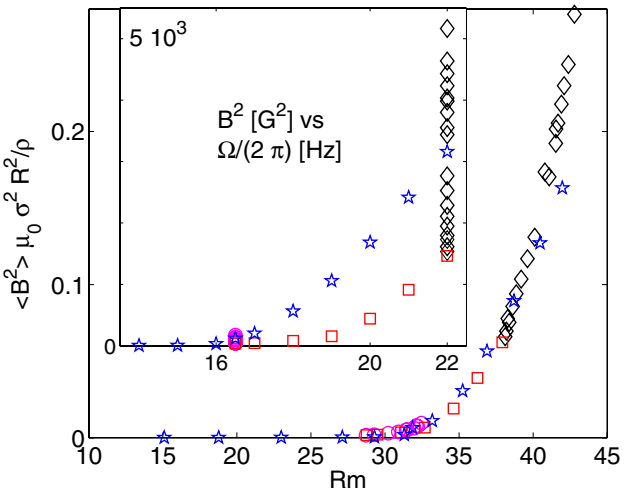

FIG. 4 (color online). The dimensionless quantity, $\langle B^2\rangle\mu_0(\sigma R)^2/\rho$ is displayed as a function of R_m for different working temperatures and frequencies [measurements done at $P2$ and identical symbols as in the inset of Fig. 3(b)]. The inset shows the same data in dimensional form B^2 versus rotation frequency for different temperatures.

perature range but the predicted order of magnitude for $\langle B^2 \rangle$ would be 10^5 too small.

Dissipated power by Ohmic losses is another important characterization of dynamo action. Our measurements show that, 30% above threshold, it leads to an excess power consumption of 15%–20% with respect to a flow driving power of the order of 100 kW.

The effect of iron disks deserves additional discussion. A slight effect of magnetization of iron has been observed: the dynamo threshold during the first run was about 20% larger than in the next runs for which all the measurements were then perfectly reproducible. However, no effect of remanence that would lead to a hysteretic behavior close to the bifurcation threshold has been observed. Demagnetization of pure iron occurring for field amplitudes of the order of the Earth field, i.e., much smaller than the fields generated by the dynamo, the iron disks do not impose any permanent magnetization but mostly change the boundary condition for the magnetic field generated in the bulk of the flow. This changes the dynamo threshold and the near critical behavior for amplitudes below the coercitive field of pure iron. It should be also emphasized that the axisymmetry of the setup cannot lead to Herzenberg-type dynamos [25]. In addition, these rotor dynamos display a sharp increase of the field at threshold and their saturation is mostly limited by the available motor power [25]. On the contrary, we observe a continuous bifurcation with a saturated magnetic field in good agreement with a scaling law derived for a fluid dynamo.

The different mechanisms at work, effect of magnetic boundary conditions, effect of mean flow with respect to turbulent fluctuations, etc., will obviously motivate further studies of the VKS dynamo. A preliminary scan of the parameter space has shown that when the disks are rotated at different frequencies, other dynamical dynamo regimes are observed including random inversions of the field polarity. Their detailed description together with experiments on the relative effect of the mean flow and the turbulent fluctuations on these dynamics are currently in progress.

We gratefully acknowledge the assistance of D. Courtiade, J.-B. Luciani, P. Metz, V. Padilla, J.-F. Point, and A. Skiara and the participation of J. Burguete to the early stage of VKS experiment. This research is supported by the French institutions: Direction des Sciences de la Matière and Direction de l'Energie Nucléaire of CEA, Ministère de la Recherche and Centre National de Recherche Scientifique (No. ANR NT05-1 42110, GDR 2060). The experiments have been realized in CEA/Cadarache-DEN/DTN.

*Present address: LEGI, CNRS UMR 5519, BP53, 38041 Grenoble, France.

†Present address: IFREMER, Laboratoire de Physique des Océans, CNRS UMR 5519, BP70, 29280 Plouzane, France.

‡Present address: Laboratory for Aero and Hydrodynamics, TU-Delft, The Netherlands.

[1] H. K. Moffatt, *Magnetic Field Generation in Electrically Conducting Fluids* (Cambridge University Press, Cambridge, U.K., 1978).
[2] G. O. Roberts, Phil. Trans. R. Soc. A **271**, 411 (1972); Yu. B. Ponomarenko, J. Appl. Mech. Tech. Phys. **14**, 775 (1973).
[3] R. Stieglitz and U. Müller, Phys. Fluids **13**, 561 (2001); A. Gailitis *et al.*, Phys. Rev. Lett. **86**, 3024 (2001).
[4] F. H. Busse, U. Müller, R. Stieglitz, and A. Tilgner, Magnetohydrodynamics **32**, 235 (1996); K.-H. Rädler, E. Apstein, M. Rheinhardt, and M. Schüler, Studia Geophys. **42**, 224 (1998); A. Gailitis *et al.*, Magnetohydrodynamics **38**, 5 (2002).
[5] F. Pétrélis and S. Fauve, Eur. Phys. J. B **22**, 273 (2001).
[6] A. A. Schekochihin *et al.*, Phys. Rev. Lett. **92**, 054502 (2004); S. Boldyrev and F. Cattaneo Phys. Rev. Lett. **92**, 144501 (2004), and references therein.
[7] J.-P. Laval *et al.*, Phys. Rev. Lett. **96**, 204503 (2006).
[8] Y. Ponty *et al.*, Phys. Rev. Lett. **94**, 164502 (2005); Y. Ponty *et al.*, Phys. Rev. Lett. (to be published).
[9] H. C. Nataf *et al.*, Geophys. Astrophys. Fluid Dyn. **100**, 281 (2006).
[10] P. Odier, J. F. Pinton, and S. Fauve, Phys. Rev. E **58**, 7397 (1998); N. L. Peffley, A. B. Cawthorne, and D. P. Lathrop, Phys. Rev. E **61**, 5287 (2000); E. J. Spence *et al.*, Phys. Rev. Lett. **96**, 055002 (2006); R. Stepanov *et al.*, Phys. Rev. E **73**, 046310 (2006).
[11] M. Bourgoin *et al.*, Phys. Fluids **14**, 3046 (2002); F. Pétrélis *et al.*, Phys. Rev. Lett. **90**, 174501 (2003); R. Volk *et al.*, Phys. Rev. Lett. **97**, 074501 (2006).
[12] L. Marié and F. Daviaud, Phys. Fluids **16**, 457 (2004).
[13] Induction experiments with only one disk driving liquid sodium have been performed by B. Lehnert, Ark. Fys. **13**, 109 (1957); another rapidly rotating flow geometry has been proposed by F. Winterberg, Phys. Rev. **131**, 29 (1963).
[14] F. Ravelet *et al.*, Phys. Fluids **17**, 117104 (2005).
[15] F. Ravelet, Ph.D. thesis, Ecole Polytechnique, 2005 [http://www.imprimerie.polytechnique.fr/Theses/Files/Ravelet.pdf].
[16] R. Volk *et al.*, Phys. Fluids **18**, 085105 (2006).
[17] F. Pétrélis and S. Fauve, Europhys. Lett. **76**, 602 (2006).
[18] S. Fauve and F. Pétrélis, in *The Dynamo Effect*, edited by J.-A. Sepulchre Peyresq Lectures on Nonlinear Phenomena Vol. II (World Scientific, Singapore, 2003), pp. 1–64.
[19] R. Avalos-Zuniga, F. Plunian, and A. Gailitis, Phys. Rev. E **68**, 066307 (2003).
[20] F. Stefani *et al.*, Eur. J. Mech. B, Fluids **25**, 894 (2006).
[21] R. Berthet *et al.*, Physica (Amsterdam) **174D**, 84 (2003).
[22] D. Sweet *et al.*, Phys. Rev. E **63**, 066211 (2001).
[23] S. Aumaître, F. Pétrélis, and K. Mallick, Phys. Rev. Lett. **95**, 064101 (2005).
[24] F. Pétrélis and S. Aumaître, Eur. Phys. J. B **51**, 357 (2006).
[25] F. J. Lowes and I. Wilkinson, Nature (London) **198**, 1158 (1963); **219**, 717 (1968).